New archaeointensity data from Italy and geomagnetic field intensity variation in the Italian Peninsula

E. Tema, J. Morales, A. Goguitchaichvili, Pierre Camps

Geophysical Journal International

Geophys. J. Int. (2013) **193,** 603–614 doi: 10.1093/gji/ggs120

New archaeointensity data from Italy and geomagnetic field intensity variation in the Italian Peninsula

E. Tema,[1,2] J. Morales,[3] A. Goguitchaichvili[3,*] and P. Camps[4]

[1] *Dipartimento di Scienze della Terra, Università degli Studi di Torino, via Valperga* 35, 10125, *Torino, Italy. E-mail: evdokia.tema@unito.it*
[2] *ALP-Alpine Laboratory of Palaeomagnetism, via G.U. Luigi Massa* 6, 12016, *Peveragno, Italy*
[3] *Laboratorio Interinstitucional de Magnetismo Natural, Instituto de Geofisica, UNAM, Campus Morelia, Michoacan, Mexico*
[4] *Géosciences Montpellier, CNRS and Université Montpellier* 2, *Montpellier, France*

Accepted 2012 December 21. Received 2012 December 20; in original form 2012 September 12

SUMMARY

We present new archaeointensity results from three Italian kilns situated at Ascoli Satriano, Vagnari and Fontanetto Po obtained with the Thellier modified by Coe double heating method. These data complement the directional results previously published. All sites are dated on the basis of archaeological information and/or thermoluminescence dating. The results are corrected for the anisotropy of the thermoremanent magnetization and the cooling rate effects. The new data are compared with previously published archaeointensity data from Italy and nearby countries within 900 km radius from Viterbo. An initial data set including archaeointensity data mainly coming from Italy, France, Switzerland, Czech Republic, Slovakia, Hungary, Greece and Bulgaria has been compiled. After the application of strict selection criteria, the most reliable data have been used for the calculation of a preliminary Italian intensity secular variation (SV) curve for the last 3000 yr. The new curve covers the 300 BC–400 AD and 1200–1900 AD periods. It is established by means of sliding windows of 200 yr shifted by 100 yr. The lack of reliable data for the 1000–200 BC and 400–1200 AD time intervals does not permit the calculation of a continuous curve. Clearly, more high-quality archaeointensity data from Italy and Europe are still needed to draw a robust intensity SV curve for the Italian Peninsula that could be used for archaeomagnetic dating in combination with the directional data.

Key words: Archaeomagnetism; Palaeointensity; Palaeomagnetic secular variation.

INTRODUCTION

Palaeomagnetic records from archaeomagnetic artefacts extend the direct observations of the Earth's magnetic field, performed by satellite and geophysical observatories, through historical and archaeological times. Thanks to important progress in archaeomagnetic research during the last decades, a large number of reliable archaeomagnetic data has been added in regional (Schnepp *et al.* 2004; Gómez-Paccard *et al.* 2006; Tema *et al.* 2006) and global (Korte *et al.* 2005; Genevey *et al.* 2008; Donadini *et al.* 2009; Goguitchaichvili *et al.* 2011, 2012) data sets. Such data allow, with a good accuracy, modelling of past geomagnetic field variations (Korte & Constable 2005, 2011; Valet *et al.* 2008; Korte *et al.* 2009, 2011; Pavón-Carrasco *et al.* 2009). However, in most of the published studies up to now only two of the ancient geomagnetic field elements (declination and inclination) are retrieved. Consequently, archaeomagnetic dating is not as reliable as it could be if the full local field vector (direction and intensity) is compared with the reference secular variation (SV) curves.

In Italy, archaeological remains are abundant but archaeomagnetic studies are still scarce (Tema 2011). Tema *et al.* (2006) constructed a preliminary directional SV curve by means of Bayesian statistical modelling from 74 reference directional data. However, although archaeointensity measurements do not require *in situ* sampling, reliable archaeointensity results in Italy are very limited and less numerous than the directional data. Their limited number has not permitted up to now the construction of a continuous and detailed intensity SV reference curve (Tema *et al.* 2010) and makes critical the need of new high-quality intensity records.

We present here new archaeointensity results from three Italian kilns with ages ranging from 300 to 1900 AD. These new absolute intensity data are obtained by Coe's modified Thellier method (Thellier & Thellier 1959; Coe 1967) including regular partial thermoremanent magnetization (pTRM) and pTRM tail checks. The effects of TRM anisotropy and cooling rate upon TRM acquisition

* Now at: Laboratorio de Paleomagnetismo, Departamento de Física, Escuela Politécnica Superior, Universidad de Burgos, C/Francisco de Vitoria, s/n, 09006, Burgos, Spain.

were investigated for all specimens. The new data can be considered as reliable markers of the past geomagnetic field intensity in Italy and enhance the European archaeointensity data set. These data together with the archaeointensity results included in a 900-km circle around Viterbo (42.45°N, 12.03°E) have been used for the calculation of a preliminary intensity SV curve for the Italian peninsula covering the 300 BC–400 AD and 1200–1900 AD time intervals.

ARCHAEOLOGICAL SITES AND SAMPLES

The studied materials are bricks coming from three archaeological kilns excavated at Ascoli Satriano (Puglia, southern Italy), Vagnari (Puglia, southern Italy) and Fontanetto Po (Vercelli, northern Italy) (Fig. 1).

Archaeomagnetic sampling of the kiln excavated at the archaeological site of Faragola, Ascoli Satriano was carried out on 2003 July in collaboration with the archaeologists Prof Giuliano Volpe and Dr Maria Turchiano (Università di Foggia). The excavation of Faragola is located a few kilometres NW of Ascoli Satriano (Lat. = 41.21°, Long. = 15.56°) in the province of Foggia (southern Italy). The archaeological excavation revealed an extended rural settlement dominated by a luxurious Roman villa, rich in decoration, marble pavement and colourful mosaics. The kiln sampled was excavated just few metres away from the villa and it is considered as a small part of a wider group of workshop structures. It was constructed by a mixture of clay and brick fragments that were incorporated into the structure. The excavation brought into light the combustion chamber and baking floor, while the firing chamber and the dome of the kiln were not preserved. We collected five brick hand samples from the baking floor of the kiln. Each brick was oriented *in situ* with a magnetic and a solar compass. According to archaeological evidence, the kiln was probably used to produce bricks for the construction of the nearby Roman villa. It is archaeologically dated around 350–400 AD.

The archaeological site of Vagnari (Lat. = 40.83°, Long. = 16.27°) is located around 12 km south of Gravina, in Apuglia region, southern Italy. It is considered as the largest site and the main economic centre in Gravina's valley dated to the Roman Imperial period. Excavation of the site began in 2000 directed by Dr Alastair Small from the University of Edinburgh in collaboration with British, Italian, American and Canadian archaeologists. Excavations carried out in several years revealed the presence of a settlement consisting of housing, as well as a large industrial zone, comprising four tile kilns, smithies and a block of workshops. The kiln sampled was excavated in Trench 5 during the excavation of 2001 July and it was almost attached to a much larger kiln

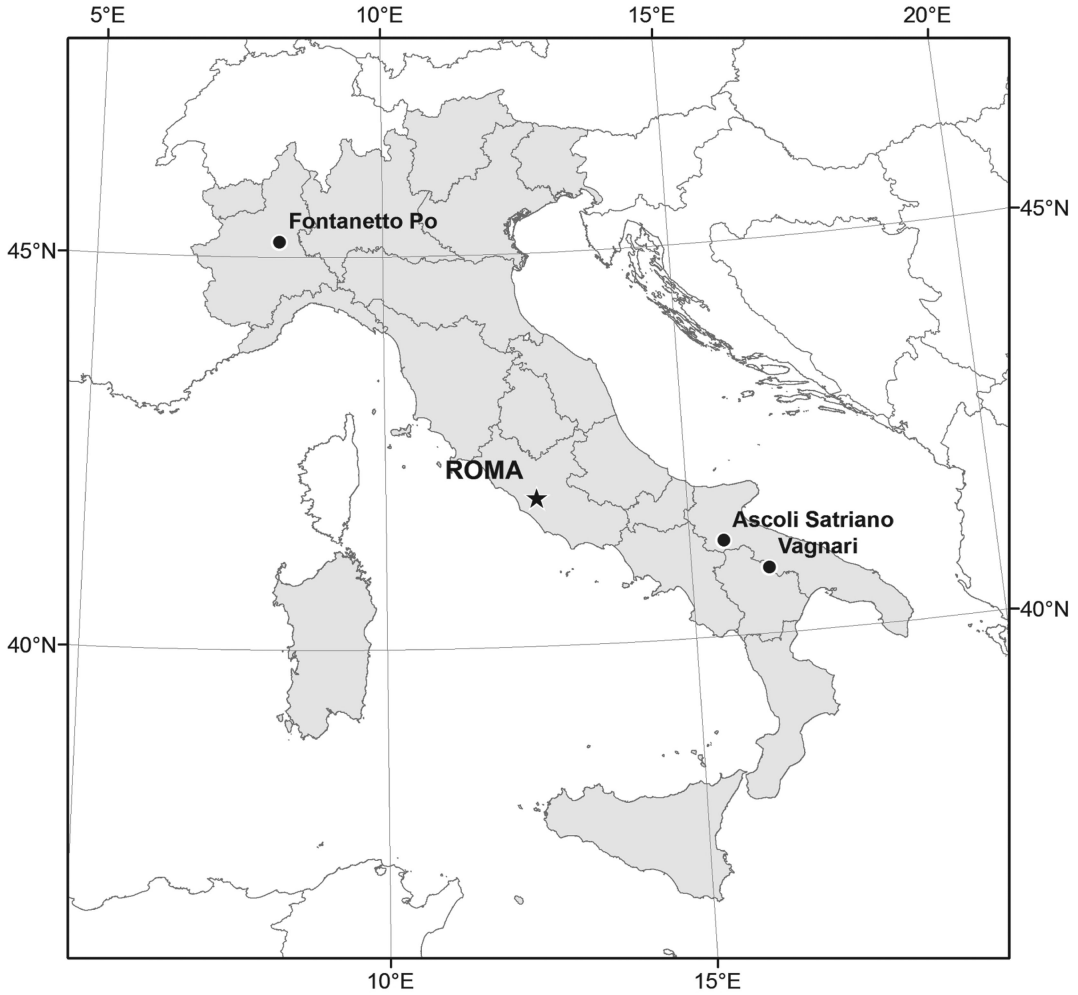

Figure 1. Location of the new sites.

excavated a year before (kiln in Trench 4 excavated on 2000 July). It is a small kiln built in a cavity dug into the natural clay which formed the floor and the lower part of the walls up to the level of the brick arches that supported the firing chamber. The walls in the interior of the combustion chamber are preserved to a maximum height of 80 cm. Their upper parts are formed by tiles and bricks laid in courses with their edges outwards; four courses survive in the best preserved wall opposite the praefurnium. To sample this structure in 2003 July, its partial re-excavation was necessary, as the trench was backfilled with soil at the end of the excavation of 2001 July. This partial re-excavation brought to light only half of the kiln, but it made possible the collection of brick fragments from the western wall of the combustion chamber. Nine hand samples were collected and oriented in the field with an inclinometer and both magnetic and solar compasses. Excavation of the Trench 5 provided archaeological evidence for the age of the kiln based on radiocarbon dating and also on ceramic findings. A piece of charcoal from the stokehole of the smaller kiln (archaeological layer 64) has a radiocarbon date of 1775 $\pm$ 45 BP, which yields calibrated dates of 210–340 AD at 59.4 per cent probability and 130–390 AD at 95.4 per cent probability (A. Small, 2004, personal communication). This age corresponds to the death of the wood found in the kiln that is not necessarily identical to the age of the kiln itself. A fragment of pottery found in the lower fill of the combustion chamber is radiocarbon dated at 230–325 AD and pieces of an African red slip found in the upper layer of the fill of the stokehole are datable at 350–400 AD. This information suggests that the kiln was not filled before the late fourth century AD and according to the archaeologists can be safely dated around 300–400 AD.

The third studied kiln was excavated near to the small village of Fontanetto Po, Vercelli Province, northern Italy, at the locality called Mulino San Giovanni (45.19°N, 8.19°E). It is a large, rectangular kiln, unearthed during a rescue excavation for the installation of methane gas pipelines. In the vicinity of the sampled kiln, at least three other kilns have been identified and according to the archaeologists they probably were part of an important workshop for the production of bricks in the area (Barello *et al.* 2012). The kiln was constructed by several series of bricks. According to the archaeologists, the kiln was in use during mediaeval times but no ceramic fragments or other archaeological findings exist to permit a more precise archaeological dating. Thermoluminescence dating on two bricks from the kiln structure suggests that the kiln's last firing occurred at 1796–1914 AD (Tema *et al.*, 2013). For this study, 23 brick samples have been collected from the kiln walls and have been oriented *in situ* using an inclinometer. The metallic methane pipelines already situated at a depth of around 1 m below the structure prevented the reliable use of a magnetic compass and the wooden and plastic protection coverage mounted to protect the kiln from adverse weather conditions hampered the use of sun compass.

In all cases, the block samples collected in the field were then drilled in the laboratory using an electric water-cooled rock drill to obtain cylindrical specimens of standard dimensions (diameter = 25.4 mm, height = 22 mm). Almost all samples were drilled perpendicular to their flat surface, interpreted as the top or the bottom of the brick. A part of the prepared samples have been previously used for archaeomagnetic directional studies and the directional results from Ascoli Satriano and Vagnari kilns as well as those from Fontanetto Po kiln are published by Tema *et al.* (2006) and Tema *et al.* (2013) respectively. In this study, a total of 54 specimens from the three kilns (11 from Ascoli Satriano, 21 from Vagnari and 22 from Fontanetto Po) have been used for archaeointensity determination.

MAGNETIC MINERALOGY

Magnetic mineralogy experiments have been done at the ALP Palaeomagnetic laboratory (Peveragno, Italy) and at the Palaeomagnetic laboratory of Thessaloniki (Greece). Low-field magnetic susceptibility versus temperature experiments, isothermal remanent magnetization (IRM) acquisition curves and thermal demagnetization of three orthogonal IRM components (Lowrie 1990) have been used for the evaluation of the thermal stability of the samples and the identification of the main magnetic minerals. The temperature dependence of low-field magnetic susceptibility from ambient temperature up to 700 °C was monitored with a Bartington MS2B susceptibility meter in combination with an MS2WF heating unit. Thermomagnetic curves are useful indicators for the thermal stability of baked materials and thus for the suitability of the material for archaeointensity determinations. For all studied sites, the obtained heating and cooling curves, even if sometimes characterized by different shapes, are almost always reasonably reversible (Fig. 2). They indicate that no substantial magnetomineralogical changes take place during heating and suggest that the bricks are magnetically stable.

We determined the coercive force properties of some selected samples at the ALP Palaeomagnetic laboratory using an ASC pulse magnetizer for imparting the IRM and a JR6 spinner magnetometer (AGICO) for measuring acquisition curves of IRM. Stepwise magnetic fields up to 1.6 or 1.8 T were applied. Samples from all sites have similar magnetic properties. The IRM curves indicate that the saturation of the magnetization is generally reached at low fields varying from 0.2 to 0.4 T indicating the presence of a low-coercivity mineral such as magnetite (Fig. 3). Only few samples from Fontanetto Po kiln (e.g. samples F14 and F19) remain unsaturated above 1.8 T and contain contributions of high-coercivity mineral, probably haematite. These results are confirmed by thermal demagnetization experiments of a three-component IRM (Lowrie 1990). Magnetization was induced along the three sample axes, applying first the maximum field (1.6 T) along the cylinder Z-axis, then the intermediate field (0.5 T) along the *Y*-axis and finally the minimum field (0.1 T) along the *X*-axis. The demagnetization curves (Fig. 4) show the dominance of the magnetically soft fraction ($<$0.1 T) with unblocking temperatures ranging between 460 and 520 °C. In few samples from Fontanetto Po, the presence of a small fraction of medium and/or high coercivity mineral is also observed. These results point to magnetite or Ti-magnetite as the main magnetic carrier in the studied samples, with some small content Ti-haematite in some cases.

ARCHAEOINTENSITY DETERMINATION

All archaeointensity measurements have been carried out at the LIMNA palaeomagnetic laboratory of UNAM (Campus Morelia, Mexico) with the classical Thellier method (Thellier & Thellier 1959) as modified by Coe (Coe 1967; Coe *et al.* 1978). Samples were heated and cooled in an ASC Scientific TD48-SC furnace and the remanence was measured with a JR5 spinner magnetometer. All heating/cooling cycles were performed in air. 10 temperature steps were distributed from 25 to 540 °C. The direct laboratory field of 30.00 $\pm$ 0.05 μT was applied during heating and cooling along the cylindrical axis (*Z*) of the samples. Every three temperature steps a pTRM check was performed to detect any change in the pTRM acquisition capacity. Additional pTRM tail checks were performed at two intermediate temperatures (350 and 450 °C).

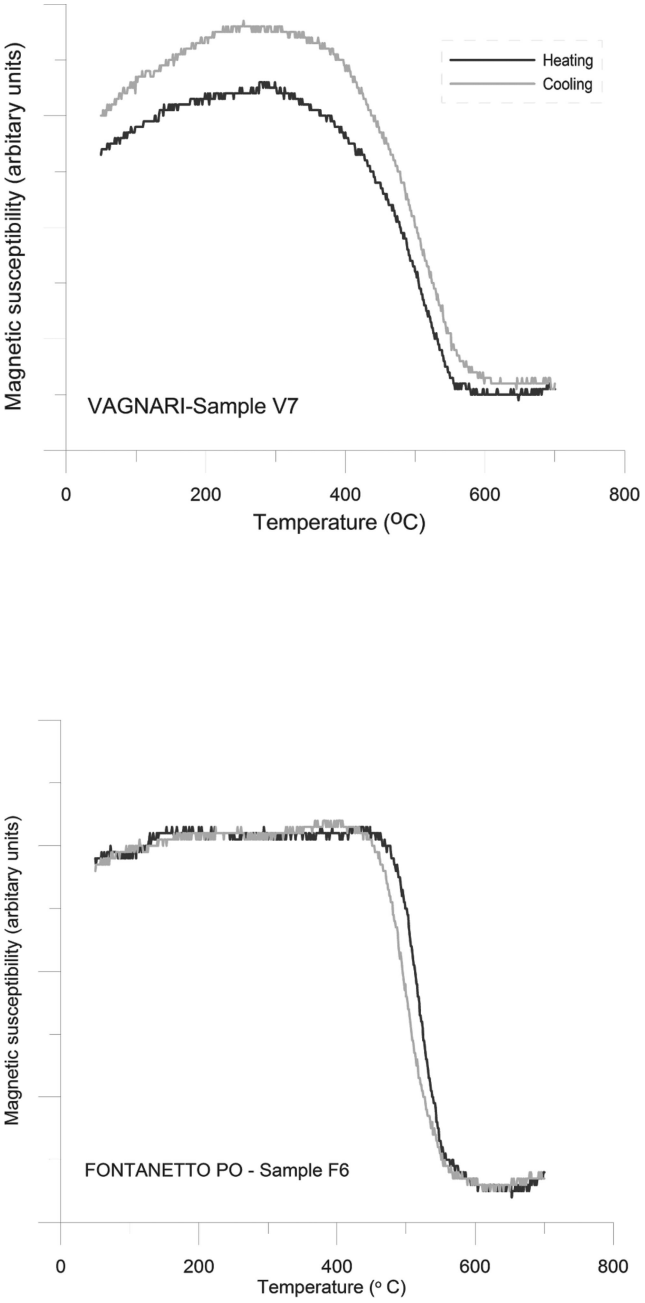

Figure 2. Representative continuous magnetic susceptibility versus temperature curves.

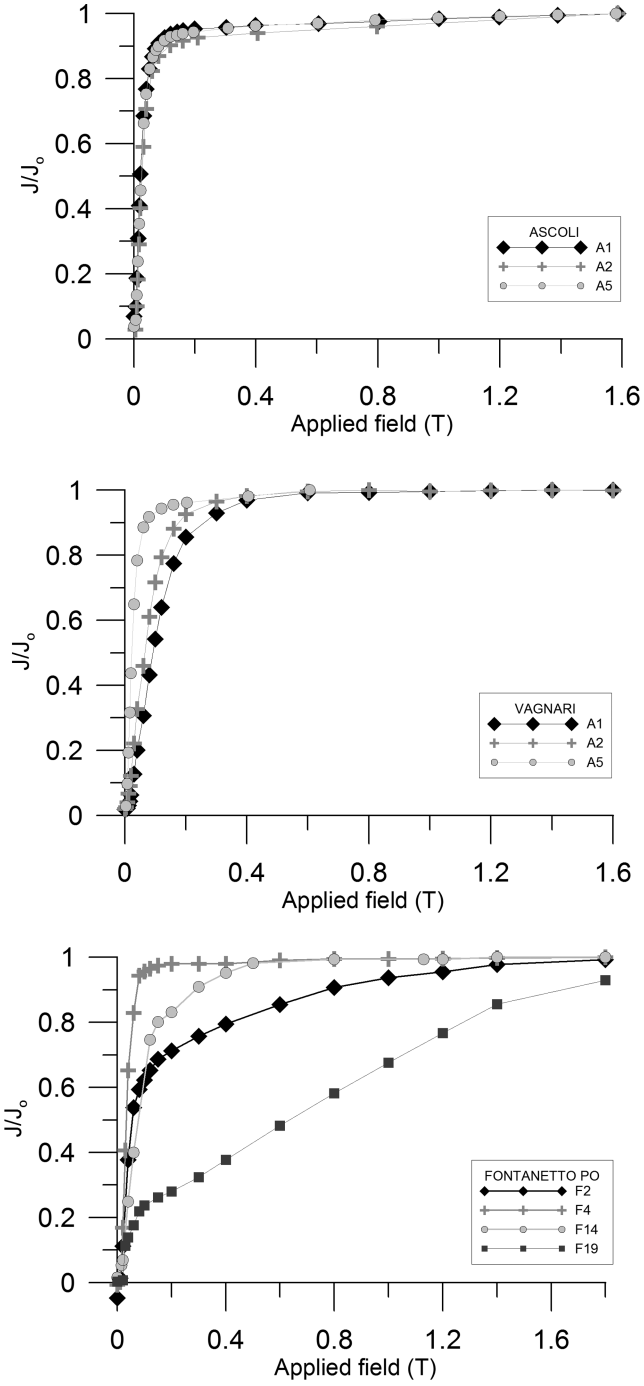

Figure 3. Representative normalized IRM acquisition curves for samples from Ascoli Satriano, Vagnari and Fontanetto Po kilns.

During the Thellier experiments, the cooling time (using a TD48 thermal demagnetizer with fan on) ranges from 30 to 45 min. According to archaeological information, the natural cooling time in ancient kilns is much higher and can range from 6 to 10 hr. It has been shown, both from theoretical considerations (Néel 1949; Halgedahl *et al.* 1980; McClelland-Brown 1984) and from experimental studies (e.g. Fox & Aitken 1980) that the intensity of a TRM is significantly affected by the cooling rate of the samples. To quantify the cooling rate effect in our samples, we investigated the cooling rate dependence of TRM following a modified procedure to that described by Chauvin *et al.* (2000). At the end of the archaeointensity experiments, all specimens were heated three more times at 540 °C in the presence of the same laboratory field used during the archaeointensity determination. First, a new TRM (TRM_1) was given to all the samples created in the same conditions as that gained during the last step of the Thellier experiment. Then, a second TRM (TRM_2) was given with a longer cooling time (∼6 hr); during this procedure, specimens were left inside the oven's heating compartment and the temperature was progressively decreased (manually) to reach room temperature in approximately 6 hr. Finally, a third TRM (TRM_3) was created using the same cooling time as that used during the TRM_1 (approximately 45 min). The cooling rate factor f_{CR} was

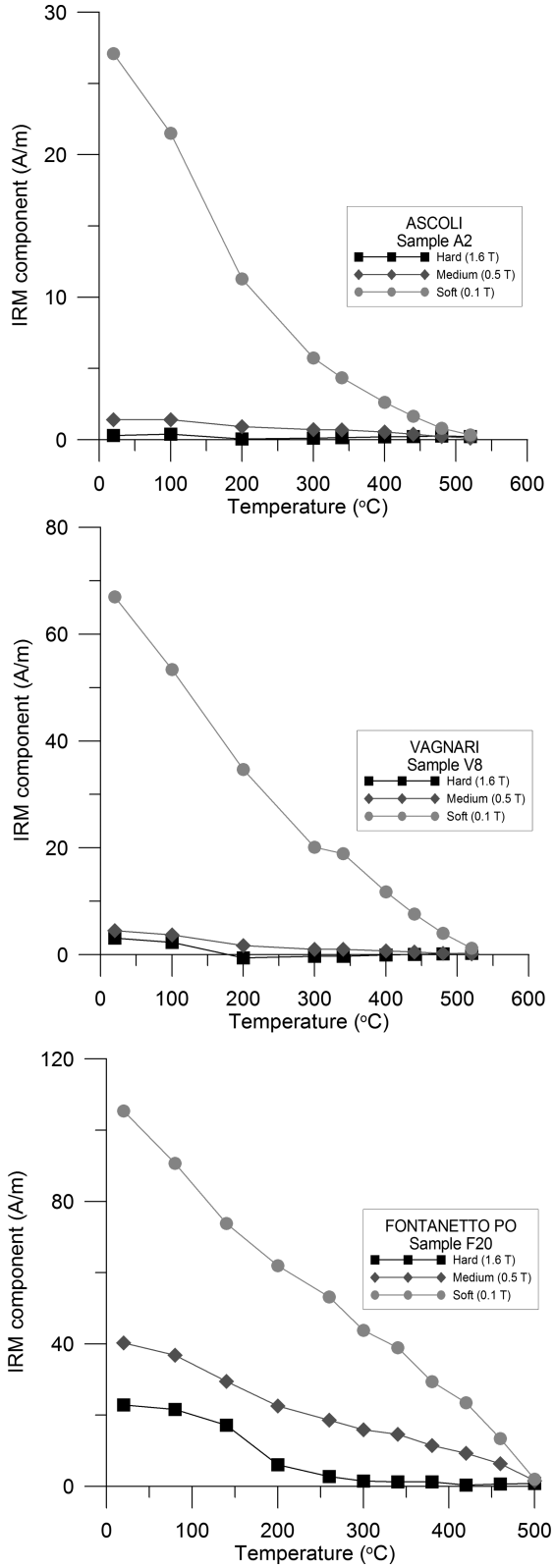

Figure 4. Stepwise thermal demagnetization of three IRM components for representative samples. Symbols: dot = low- (0.1 T); diamond = intermediate- (0.5 T); square = high- (1.6 T) coercivity component.

calculated as the variation between the intensity acquired during a short and a long cooling time: $f_{CR} = (TRM_2 - TRM_1)/TRM_2$. Changes in TRM acquisition capacity were estimated by means of the percentage variation between the intensity acquired during the same cooling time (TRM_1 and TRM_3). The cooling rate correction was applied only when the corresponding change in TRM acquisition capacity was below 15 per cent and $f_{CR} > 0$ (Morales *et al.* 2009).

Anisotropy of TRM (ATRM) measurements has been also performed to estimate the ATRM effect on the ancient geomagnetic field vector. The ATRM measurements were carried out at the palaeomagnetic laboratory of Géosciences Montpellier (France), by inducing in the sample a pTRM (540 °C to room temperature) in six directions (i.e. $+x$, $+y$, $+z$, $-x$, $-y$, $-z$) in the presence of magnetic field of 50 μT. Zero-field thermal demagnetizations at 540 °C before each pTRM were used as a baseline. These measurements were performed on the same specimens used for archaeointensity determination after the last heating step. We calculated the anisotropy correction factor for each specimen according to Veitch *et al.* (1984).

NEW ARCHAEOINTENSITY DATA FROM ITALY

Archaeointensity determinations have been performed on 54 specimens from the three studied kilns. The obtained results, interpreted using NRM–TRM plots (Fig. 5), are reported in Table 1 together with the statistical parameters calculated according to Coe *et al.* (1978). For most of the specimens, linear NRM–TRM curves and positive pTRM checks are obtained (Fig. 5). No secondary component of magnetization was detected in the directional plots obtained from the palaeointensity experiments and the viscous magnetization, if any, was easily removed at 100–150 °C. To guarantee the quality of the new results, we applied selection criteria based on the linearity of the NRM–TRM diagrams, the Coe's quality parameters (Coe *et al.* 1978) and the pTRM checks. According to this selection, all the accepted new results fulfil the following criteria:

- The Arai diagrams, in which the NRM remaining is plotted against the TRM acquired after each heating step, are linear and the number of the aligned points (N) used for the calculation of the archaeointensity is $\geq$5. Only archaeointensities with NRM fraction factor (f, Coe *et al.* 1978) $\geq$0.3 are accepted; this means that at least the 30 per cent of the initial NRM was used for their determination.
- No significant deviation of the NRM directions towards the applied field is observed, as revealed in the vector (Zijderveld) plots. Archeointensity results obtained from NRM–pTRM diagrams must show no evident concave up shape, since in such cases remanence is probably associated with the presence of MD grains (Levi 1977; Kosterov *et al.* 1998).
- Only results with positive pTRM checks are accepted for which the deviation of the pTRM checks is less than 15 per cent. Evaluation of pTRM tail checks performed at two different temperatures is in most cases lower than 20 per cent (Ascoli Satriano and Vagnari) and 30 per cent (Fontanetto Po).

To guarantee the high quality of the new results, the mean site intensities were calculated only from specimens that were corrected for both cooling rate and ATRM effects. Three new reliable mean site intensities have been obtained for Italy; Ascoli Satriano (350–400 AD): 53.8 ± 3.7; Vagnari (300–400 AD): 52.8 ± 4.4; Fontanetto Po (1796–1914 AD): 45.9 ± 2.6 μT.

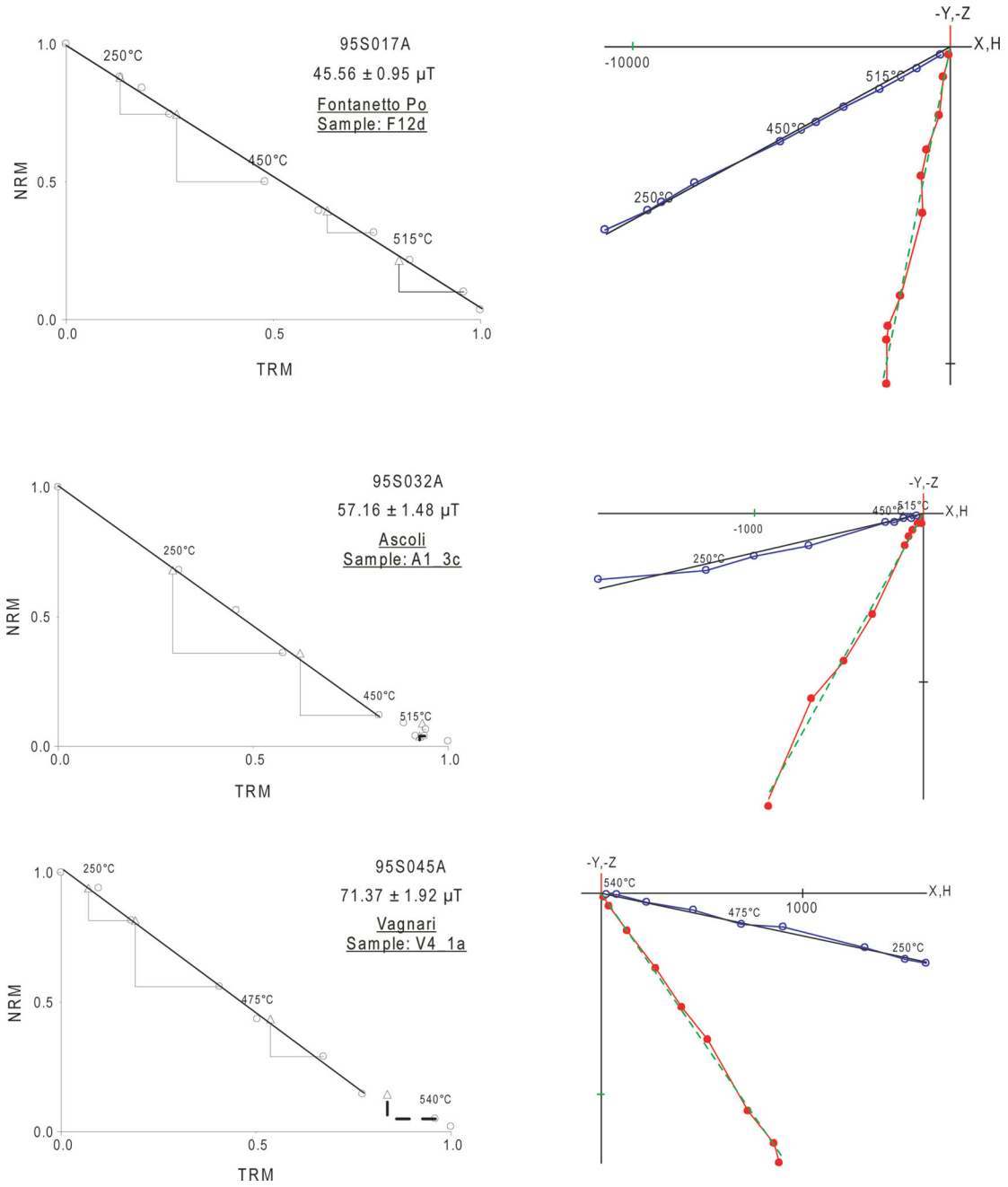

Figure 5. Examples of NRM–TRM plots and corresponding orthogonal vector projections of the remanent magnetization in sample coordinates from successful archaeointensity experiments. Diagrams are normalized to the initial NRM intensity. In the orthogonal projections, the open (closed) dots refer to inclinations (declinations). During intensity experiments, regular pTRM checks were performed (triangles in the NRM/TRM diagrams).

COMPARISON WITH ARCHAEOINTENSITY RESULTS FROM ITALY AND EUROPE AND GEOMAGNETIC FIELD INTENSITY VARIATION IN THE ITALIAN PENINSULA

Archaeointensity data from Italy are very limited, and up to now only 23 intensity results have been published coming from archaeological artefacts (Tema 2011). More intensity data coming from volcanic rocks (mainly lava flows from Vesuvius and Etna) are available but they are mostly concentrated at the last four centuries while older periods are very poorly covered (Tema *et al.* 2010). To compare our new results with previously published Italian data for the last 3000 yr, the new intensities have been relocated at the latitude of Viterbo (42.45°N) through the virtual axial dipole moment (VADM). Lanza & Zanella (2003) proposed Viterbo (about 70 km from Rome) as the optimum reference point for relocating the directional Italian SV data as it is characterized by the smallest systematic relocation error in both declination and inclination (±0.3°), wherever the original site is situated in Italy. Following this suggestion, Viterbo has been constantly used as the common reference point by Tema *et al.* (2006) and (2010) for relocating both directional and intensity data. In Fig. 6, all data are plotted versus time together with the intensity

Table 1. New archaeointensity results at specimen level. Columns: Site; Specimen; Tmin-Tmax, minimum and maximum temperatures used for the intensity determination; *N*, the number of heating steps used for the intensity determination; slope, slope of the best fit; β, ratio of the standard error of the slope to the absolute value of the best-fitting slope for the data on the NRM–TRM diagram; *f*, the fraction of NRM used for intensity determination; *g*, the gap factor; *q*, the quality factor as defined by Coe *et al.* (1978); Mad, maximum angular deviation, Drat, difference ratio as defined by Selkin & Tauxe (2000); f_{ATRM}, magnetic anisotropy correction factor; f_{CR}, cooling rate correction factor; *F*, Palaeointensity in μT before any correction; *SD*, standard deviation in μT; F_{atrm}: Palaeointensity in μT after TRM anisotropy correction; $F_{atrm+cr}$: Palaeointensity in μT after ATRM and cooling rate correction; *Specimens in italics were rejected and therefore not used for the calculation of the site mean.*

Site	Specimen	Tmin – Tmax (°C)	*N*	slope	*b*	*f*	*g*	*q*	Mad	Drat	f_{ATRM}	f_{CR}	*F* (μT)	*SD* (μT)	*F* atrm corr	*F* atrm+cr corr
Fontanetto Po	F1B2	20–560	10	−1.53	0.03	0.95	0.75	25.6	2.1	3.2	0.981	0.027	46.0	1.3	45.1	43.9
	F1C1	20–560	10	−1.51	0.04	0.90	0.74	16.2	1.5	4.3	0.952	0.024	45.3	1.9	43.1	42.1
	F2B2	*20–560*	*10*	*−1.46*	*0.04*	*0.98*	*0.73*	*18.9*	*1.4*	*4.0*	*0.983*	*TRM_{1-3} > 15 %*	*43.7*	*1.7*	*42.9*	
	F3A2	20–515	8	−1.54	0.03	0.72	0.84	22.2	2.3	1.5	1.017	0.065	46.1	1.3	46.9	43.9
	F3C1	20–450	5	−1.57	0.06	0.89	0.69	9.9	1.5	4.1	1.008	−0.006	47.0	2.9	47.3	
	F5A2	20–475	6	−1.60	0.03	0.65	0.77	18.4	3.5	1.7	0.991	0.088	48.1	1.3	47.7	43.5
	F5A3	20–560	10	−1.62	0.02	0.96	0.84	37.4	2.5	2.3	0.987	0.076	48.7	1.1	48.1	44.4
	F6A2	250–475	5	−1.78	0.02	0.52	0.66	14.5	3.0	1.5	0.973	0.105	53.6	1.3	52.1	46.6
	F7B2	*rejected*														
	F7C1	20–350	4	−1.71	0.05	0.55	0.49	5.1	2.7	1.9	0.975	0.026	51.2	2.7	49.9	48.6
	F8A2	20–515	8	−1.80	0.04	0.88	0.75	15.8	2.9	2.5	0.999	0.105	53.9	2.3	53.8	48.2
	F9B1	20–515	8	−1.67	0.01	0.87	0.79	71.0	1.6	2.5	1.012	0.123	50.1	0.5	50.7	44.5
	F9C1	20–515	8	−1.85	0.03	0.83	0.82	20.6	3.6	3.5	0.969	0.091	55.5	1.8	53.8	48.9
	F9C2	20–560	10	−1.94	0.03	0.96	0.85	27.7	3.8	3.7	0.936	0.132	58.3	1.7	54.6	47.4
	F11B1	20–450	5	−1.65	0.03	0.52	0.67	11.7	2.3	0.6	0.988	0.104	49.5	1.5	48.9	43.8
	F12C1	20–540	9	−1.63	0.01	0.95	0.85	56.2	1.8	1.6	0.984	0.079	48.9	0.7	48.1	44.3
	F12D	20–560	10	−1.52	0.02	0.96	0.86	39.6	1.6	1.3	1.103	0.050	45.6	1	50.3	47.8
	F16A2	*350–560*	*7*	*−1.26*	*0.07*	*0.46*	*0.51*	*3.4*	*1.2*	*14.8*	*0.965*	*0.000*	*37.8*	*2.6*	*36.5*	
	F17B1	20–350	4	−1.69	0.05	0.63	0.61	8.0	6.4	1.4	1.005	−0.005	50.6	2.4	50.9	
	F18C1	20–350	4	−1.73	0.02	0.57	0.48	17.8	1.9	0.5	0.981	−0.012	52.0	0.8	51.0	
	F19C1	20–350	4	−1.78	0.04	0.60	0.34	5.7	3.2	0.4	0.970	0.016	53.5	1.9	51.9	51.1
	F21A	20–540	9	−1.53	0.07	0.97	0.75	9.9	2.8	9.5	0.952	−0.007	45.8	3.4	43.6	
	Site mean:				$F \pm SD = 50.0 \pm 3.7\ \mu T$						$F_{atrm} \pm SD = 49.4 \pm 3.3\ \mu T$			$F_{atrm+cr} \pm SD = 45.9 \pm 2.6\ \mu T$		
Ascoli Satriano	*A1–1A*	*350–560*	*7*	*−1.55*	*0.10*	*0.40*	*0.55*	*2.2*	*2.9*	*28.1*	*1.091*	*−0.413*	*46.5*	*4.7*	*50.7*	
	A1–2B	20–540	8	−1.96	0.01	0.98	0.66	47.6	3.1	1.9	1.019	−0.422	58.9	0.8	60.0	
	A1–3C	20–450	5	−1.91	0.03	0.88	0.72	24.6	3.5	2.5	1.052	−0.390	57.2	1.5	60.1	
	A2–1A	20–475	6	−2.06	0.04	0.88	0.73	18.1	4.7	1.0	0.948	−0.359	61.8	2.2	58.6	

Table 1. (*Continued.*)

Site	Specimen	Tmin – Tmax (°C)	*N*	slope	*b*	*f*	*g*	*q*	Mad	Drat	f_{ATRM}	f_{CR}	*F* (μT)	*SD* (μT)	*F* atrm corr	*F* atrm+cr corr
	A5–1A	20–560	9	−1.92	0.04	0.96	0.74	16.9	2.7	12.7	1.085	−0.376	57.7	2.4	62.6	
	A5–2B	20–560	10	−1.66	0.04	0.99	0.81	21.2	2.1	3.4	1.172	−0.024	49.7	1.9	58.2	
	A5–3C	20–475	5	−1.91	0.05	0.87	0.70	11.3	3.5	0.1	1.070	−0.070	57.2	3.1	61.2	
	A2–1A	20–475	6	−2.06	0.02	0.91	0.75	32.8	3.7	1.7	0.951	0.019	61.9	1.3	58.9	57.8
	A2–2B	20–560	10	−1.88	0.05	0.95	0.79	15.5	4.5	5.1	0.981	0.030	56.4	2.7	55.3	53.6
	A2–3C	250–560	8	−1.73	0.05	0.69	0.78	10.8	1.9	6.4	0.978	0.037	51.9	2.6	50.8	48.9
	A2–4D	20–475	5	−2.04	0.02	0.91	0.69	26.2	2.1	3.0	0.933	0.037	61.2	1.5	57.1	55.0
	Site mean:				$F \pm SD = 57.4 \pm 4.0$ μT				$F_{atrm} \pm SD = 58.3 \pm 3.3$ μT				$F_{atrm+cr} \pm SD = 53.8 \pm 3.7$ μT			
Vagnari	*V1–1A*	*450–560*	*6*	*−1.69*	*0.09*	*0.690*	*0.740*	*5.4*	*3.5*	*3.3*	*1.159*	*−0.057*	*50.7*	*4.8*	*58.8*	
	V1–2B	20–560	9	−2.07	0.04	0.960	0.810	19.7	3.6	2.6	0.992	−0.064	62.2	2.5	61.7	
	V1–3C	20–560	10	−2.06	0.09	0.927	0.862	8.7	0.0	0.0	1.000	−0.026	61.8	2.8	61.8	
	V2–1A	20–560	10	−1.93	0.04	0.890	0.840	17.7	3.0	4.5	1.053	0.033	57.8	2.5	60.8	58.8
	V2–2B	20–560	10	−2.22	0.12	0.934	0.880	14.9	0.0	0.0	1.000	−0.009	66.5	3.7	66.5	
	V3–1A	20–560	9	−1.79	0.06	1.000	0.850	14.6	2.8	2.8	1.174	−0.013	57.3	3.1	67.3	
	V3–2B	*rejected*														
	V3–3C	20–515	7	−2.34	0.08	0.720	0.810	7.3	4.4	3.3	1.188	−0.276	70.2	5.6	83.4	
	V4–1A	20–515	7	−2.38	0.03	0.850	0.810	25.5	1.9	1.8	0.895	−0.284	71.4	1.9	63.9	
	V4–2B	20–475	5	−2.21	0.07	0.520	0.730	5.1	3.8	4.1	1.019	−0.130	66.5	4.9	67.7	
	V4–3C	*rejected*														
	V5–1A	*rejected*														
	V5–2B	*rejected*														
	V5–3C	20–475	5	−1.97	0.05	0.510	0.700	6.8	5.1	4.1	1.128	−0.034	59.2	3.1	66.7	
	V6–1A	*350–515*	*5*	*−1.89*	*0.05*	*0.600*	*0.720*	*9.5*	*2.1*	*2.8*	*1.133*	*TRM1–3 > 15 %*	*56.8*	*2.6*	*64.3*	
	V7–1A	*rejected*														
	V7–2B	*20–560*	*10*	*−2.40*	*0.06*	*0.980*	*0.820*	*13.3*	*2.6*	*5.4*	*1.026*	*TRM1–3 > 15 %*	*72.1*	*4.4*	*73.9*	
	V7–3C	*rejected*														
	V8F-1A	350–560	7	−1.89	0.07	0.480	0.720	5.3	4.0	51.1	0.955	0.044	56.6	3.7	54.1	51.7
	V8K-1A	450–560	6	−1.82	0.12	0.270	0.790	1.8	10.6	94.3	0.986	0.022	54.5	6.5	53.7	52.5
	V8L-1A	250–560	9	−1.62	0.04	0.700	0.820	13.4	8.6	2.6	1.027	0.033	48.6	2.1	49.9	48.3
	Site mean:				$F \pm SD = 61.1 \pm 6.7$ μT				$F_{atrm} \pm SD = 63.1 \pm 8.7$ μT				$F_{atrm+cr} \pm SD = 52.8 \pm 4.4$ μT			

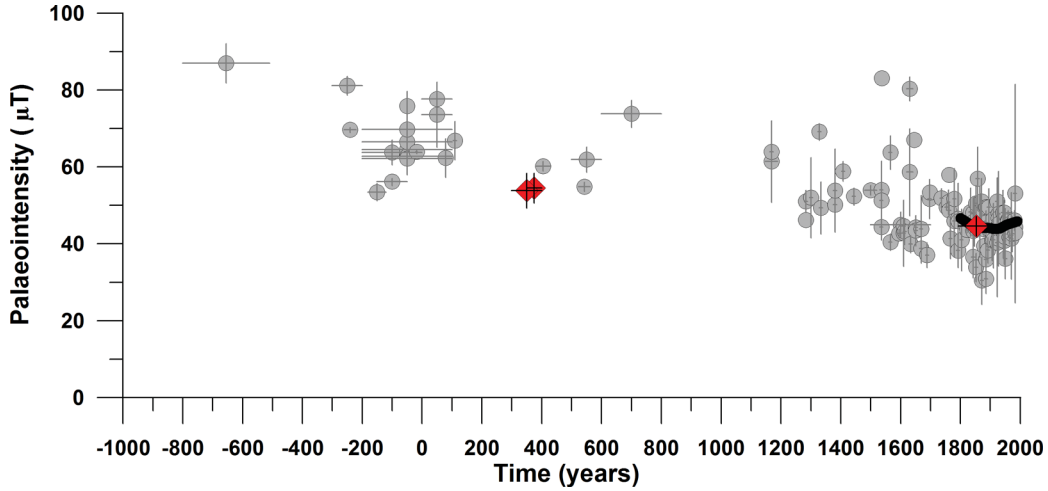

Figure 6. Italian archaeointensity data plotted versus age together with the Jackson *et al.* (2000) historical geomagnetic field model (black curve) for the last two centuries. Symbols: diamonds = new data; grey dots = data from literature.

curve for the last two centuries derived from the historical geomagnetic field model of Jackson *et al.* (2000). The archaeointensity determined from Fontanetto Po kiln is in very good agreement with the direct intensity measurements available for the last 200 yr (Jackson *et al.* 2000). The new results from Vagnari and Ascoli Satriano can be compared with the only archaeointensity result available for the 300–500 AD period that come from the study of a tile from the archaeological site of Carlino, dated around 380–430 AD (Hedley & Wagner 1991). There is a reasonable agreement between Ascoli Satriano and Carlino intensities, even though the Ascoli's intensity is slightly lower (Fig. 6). For this period, it can be noted that the new data contribute to our knowledge of the Earth's magnetic field intensity in Italy during Late Roman times.

As already discussed by Tema (2011), data coming from Italian historical volcanic eruptions show important discrepancies whereas those coming from archaeological material are still not sufficiently numerous to reliably describe the fine characteristics of the geomagnetic field's intensity variations. To increase the number of reference data (coming from Italian archaeological artefacts and volcanic rocks), we have compiled a data set including archaeointensity results from nearby to Italy countries. The GEOMAGIA V.2 global database (Donadini *et al.* 2009, available at online http://geomagia.ucsd.edu) was used to collect all available intensity data that are included in a 700-km and a 900-km radius circles around Viterbo and cover the last 3000 yr. This database has been updated with some recently published data from Greece and Tunisia (Fouzai *et al.* 2012; Tema *et al.* 2012). The 700-km circle data set still remains poor with only 42 additional data added (Fig. 7). In contrast, the 900-km data set includes 159 more archaeointensity data mainly coming from France, Switzerland, Czech Republic, Slovakia, Hungary, Greece and Bulgaria (Fig. 7). Casas & Incoronato (2007) published a detailed analysis of the distribution of the relocation errors in both direction and intensity and showed that in Europe, errors are about 0.25° per 100 km and 100–200 nT per 100 km. That means that the geographic correction of intensities from 900 km (using the VADM) could introduce relocation errors of around 0.9–1.8 μT that are negligible and in most cases are much lower than the archaeointensity measurements precision.

The 900-km data set significantly enhances the number of reference data for the Italian Peninsula and the data partially fill the gap between fourth and ninth centuries BC and first to fourth and ninth to 11th AD for which no or very few Italian data are available (Fig. 8a). Intensities from countries nearby Italy seem to be in good agreement with the Italian data particularly for the last 800 yr (1200–2000 AD) and for Roman times. For other time periods, only limited Italian data are available for comparison and in some cases discrepancies can be observed (e.g. 200–300 AD). To have a control on the quality of the reference data, quality selection criteria on the 900-km data set have been applied. As already thoroughly discussed by several authors (e.g. Donadini *et al.* 2009; Pavón-Carrasco *et al.* 2009; Tema & Kondopoulou 2011; Tema *et al.* 2012) controlling the correctness and quality of the data included in global databases is a very complicated task. The same is true for the establishment of selection criteria to collect or reject reference data. Various selection and/or ranking criteria have been proposed for the evaluation of the quality of the intensity data (Chauvin *et al.* 2000; Genevey *et al.* 2008) that are mainly based on the method used, the number of samples studied, the standard deviation, the applied anisotropy and cooling rate corrections. However, on one hand applying very strict selection criteria often results to the elimination of more than 80 per cent of the reference data (Tema & Kondopoulou 2011). On the other hand, applying soft selection criteria would allow the presence of low-quality data in the reference data set. In this study, we first applied a basic selection filter (following Tema *et al.* 2012), and we rejected all data that are characterized by age uncertainties higher than 300 yr, those that are based on less than three archaeointensity determinations and those that have standard deviations higher than 6 μT. All data that were missing the above information have also been rejected. Applying this selection filter, from the 283 initial data, 140 were rejected mainly because of the very small number of specimens/samples studied (in many cases only one). The remaining 143 data are plotted in Fig. 8(b). As it can be noted, the data are now better concentrated and some outliers previously observed around 200 AD and 450 AD are now eliminated. As a further step, we applied more severe selection criteria and we rejected all data that missed anisotropy and cooling rate corrections, taking into consideration that these corrections are very important to obtain reliable archaeointensity results, mainly in the case of pottery and brick studies. After this selection, only 51 data points remain (Fig. 8c). These data coming from Italy, France and Greece can be considered of high quality, even if limited.

For the time periods 300 BC–400 AD and 1200–1900 AD for which enough data are available, fragments of a continuous and

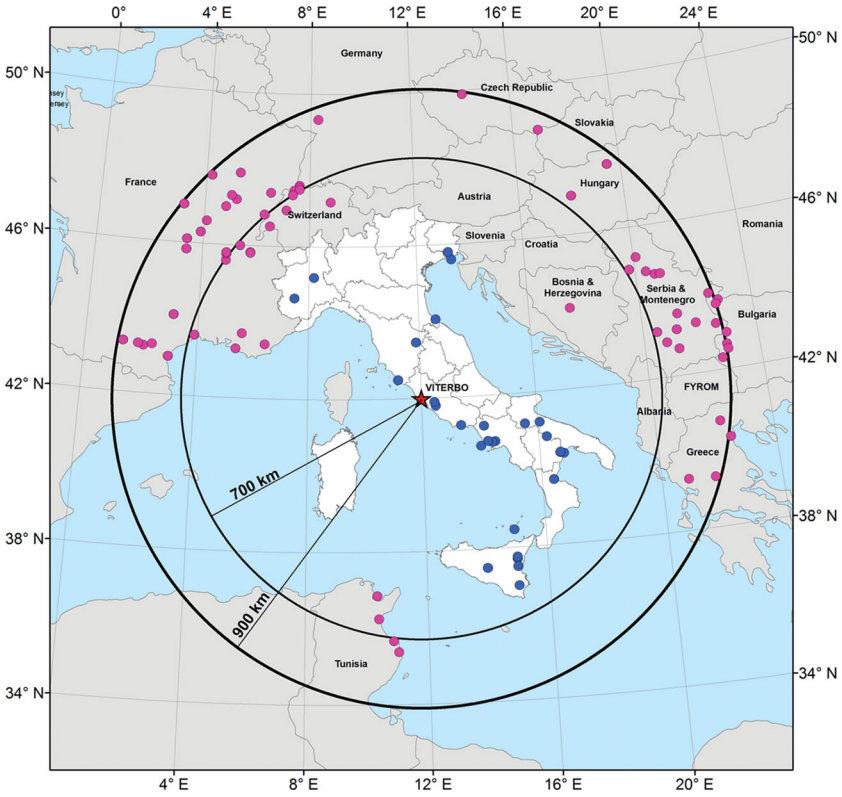

Figure 7. Geographical distribution of the archaeointensity data from Italy and nearby countries included in 700- and 900-km radius circles centred at Viterbo.

smooth SV curve were calculated using time windows of 200 yr shifted by 100 yr (Fig. 8c). A continuous Italian SV curve for the last 3000 yr cannot be calculated because of the lack of data for the 1000–200 BC and 400–1200 AD time intervals. The obtained curve fragments were compared with the results of the SCHA.DIF.3K regional geomagnetic field model (Pavón-Carrasco *et al.* 2009) and the ARCH3K global archaeomagnetic model (Korte *et al.* 2009), both calculated directly at the latitude of Viterbo (Fig. 8c). Comparison shows that the intensity curve for the Italian Peninsula is in good agreement with both regional and global models predictions for the examined time periods. These curves, based only on the most reliable data available for the area, clearly confirm that during Roman and Late Roman times (200 BC–400 AD) the intensity in Italy was stable and only very small variations around a mean intensity of 63 μT are observed. Very small intensity variations are also well registered for the 1300–1600 AD period while during the 17–18th centuries the intensity was slightly decreasing. One intensity result available from Italy for the 700 $\pm$ 100 AD (Tema *et al.* 2010) seems to be in good agreement (especially if its upper age limit is considered) with a high-intensity peak registered by the models around the eighth century AD. High intensities for this period are also observed from data from western Europe (Genevey & Gallet 2002; Gómez-Paccard *et al.* 2008) but definitely more data are necessary to investigate if this is a real feature of the geomagnetic field intensity in Europe or if it is just the result of individual erroneous high intensities due to undetected experimental problems.

CONCLUSIONS

Three new archaeointensity data have been obtained from three archaeological kilns with ages ranging from 300 to 1900 AD. Strict selection criteria have been applied to accept only the most reliable intensity determinations. The archaeointensity experiments carried out using the Thellier modified by Coe double heating method (with pTRM checks, ATRM and cooling rate corrections) give mean intensities of 53.8 $\pm$ 3.7 μT for Ascoli Satriano (350–400 AD), 52.8 $\pm$ 4.4 μT for Vagnari (300–400 AD) and 45.9 $\pm$ 2.6 μT for Fontanetto Po (1796–1914 AD). The new results are reasonably consistent with previously published Italian data and they enrich the Italian reference data set particularly for the third to fourth AD centuries. Together with other 50 strictly selected, high-quality data from Italy, France and Greece included within 900-km radius from Viterbo, they have been used for the calculation of an Italian intensity SV curve for the 300 BC–400 AD and 1200–1900 AD periods. This curve shows that during 200 BC–400 AD and 1300–1600 AD the intensity in Italian peninsula was stable whereas during the 1700–1800 AD it was slightly decreasing. This study also demonstrates that many of the previously published intensity data in Europe do not satisfy basic quality criteria and their use in the reconstruction of the past geomagnetic field variations should be very cautious. To better understand the detailed past intensity variation, it is important to obtain new high-quality archaeointensity data from Europe, and specially from Italy, particularly for the 1000–300 BC and 600–1200 AD periods that are very poorly covered by data.

ACKNOWLEDGEMENTS

ET has benefitted from the hospitality and laboratory use of the Palaeomagnetic laboratory of the Aristotele University of Thessaloniki (Greece). The reviewers Drs Elisabeth Schnepp and Simo Spassov are highly acknowledged for their useful comments on the manuscript.

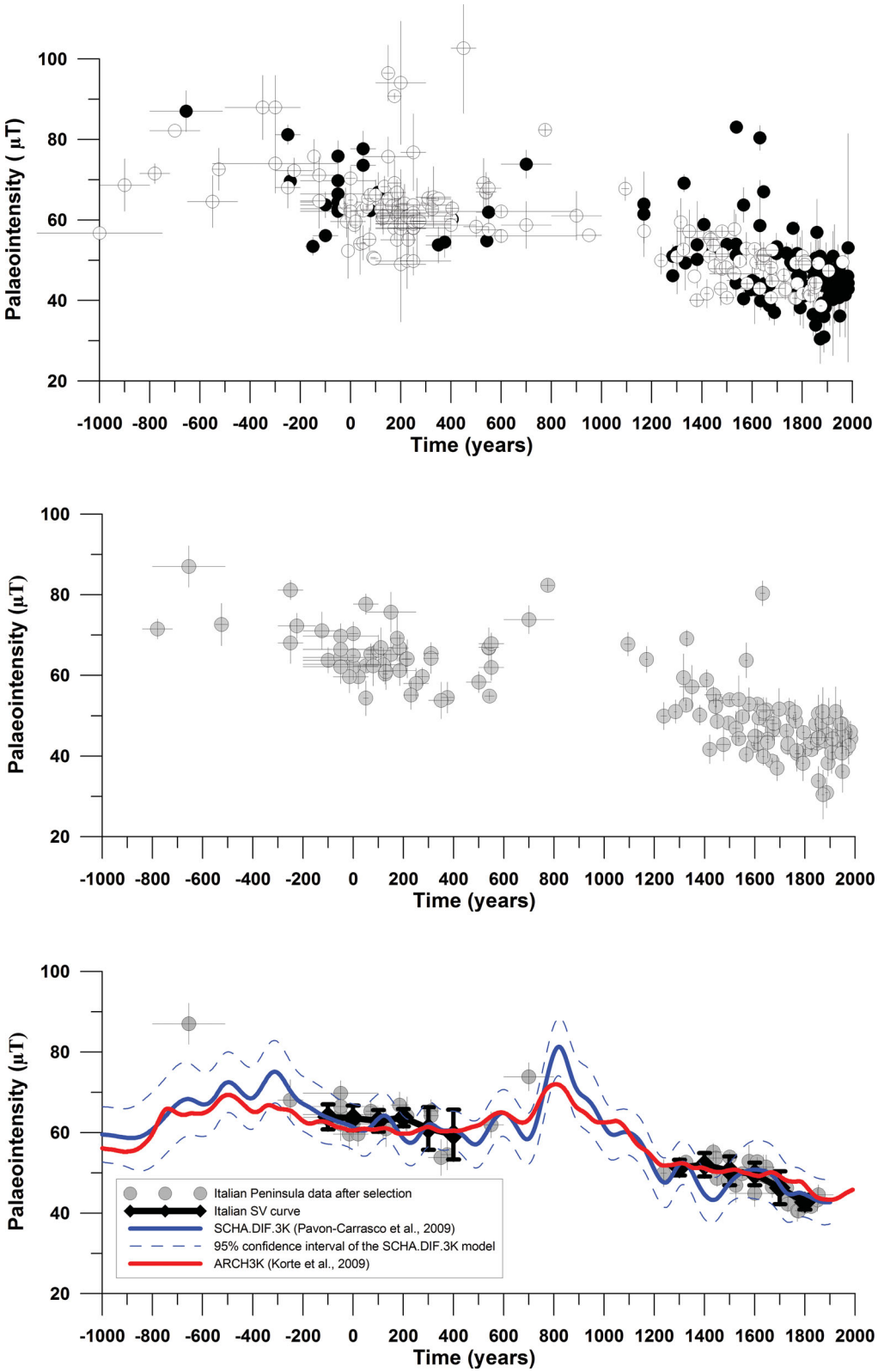

Figure 8. (a) Archaeointensity data from Italy (black dots) and from localities near Italy (white dots) included in a 900-km circle around Viterbo plotted versus time; (b) the 900-km archaeointensity data set (both from Italy and nearby countries) after the application of selection criteria based on number of specimens, age uncertainties and measurements errors (grey dots); (c) the 900-km archaeointensity data set after the application of selection criteria based also on the anisotropy and cooling rate effect corrections (grey dots) plotted together with the calculated Italian SV curve (black diamonds) and the results of the SCHA.DIF.3K regional and ARCH3K global models (see text for further explanation). All data are calculated at Viterbo (42.45°N, 12.03°E).

REFERENCES

Barello, F., Ferrara, E., Gatti, S. & Tema, E., 2012. Fontanetto Po, strada vicinale antica Torino-Casale. Fornaci di epoca moderna e strada glareata romana, *Quaderni della Soprintendenza Archeologica del Piemonte,* **27,** 242–244.

Casas, L. & Incoronato, A., 2007. Distribution analysis of errors due to relocation of geomagnetic data using the 'Conversion via Pole' (CVP) method: implications on archaeomagnetic data, *Geophys. J. Int.,* **169,** 448–454.

Chauvin, A., Garcia, Y., Lanos, Ph. & Laubenheimer, F., 2000. Paleointensity of the geomagnetic field recovered on archaeomagnetic sites from France, *Phys. Earth planet. Inter.,* **120,** 111–136.

Coe, R.S., 1967. Paleo-intensities of the Earth's magnetic field determined from Tertiary and Quaternary rocks, *J. geophys. Res.,* **72**(12), 3247–3262.

Coe, R.S., Grommé, S. & Mankinen, E.A., 1978. Geomagnetic paleointensities from radiocarbon-dated lava flows on Hawaii and the question of the Pacific nondipole low, *J. geophys. Res.,* **83**(B4), 1740–1756.

Donadini, F., Korte, M. & Constable, C.G., 2009. Geomagnetic field for 0–3 ka: 1. New data sets for global modelling, *Geochem. Geophys. Geosyst.,* **10,** doi:10.1029/2008GC002295.

Fouzai, B., Casas, L., Ouazaa, N.L. & Alvarez, A., 2012. Archaeomagnetic data from four Roman sites in Tunisia, *J. Arch. Sci.,* **39,** 1871–1882.

Fox, J.M.W. & Aitken, M.J., 1980. Cooling rate dependence of the thermoremanent magnetisation, *Nature,* **283,** 462–463

Genevey, A. & Gallet, Y., 2002. Intensity of the geomagnetic field in western Europe over the past 2000 years: new data from ancient French pottery, *J. geophys. Res.,* **107**(B11), doi:10.1029/2001JB000701.

Genevey, A., Gallet, Y., Constable, C., Korte, M. & Hulot, G., 2008. ArcheoInt: an upgraded compilation of geomagnetic field intensity data for the past ten millennia and its application to recovery of the past dipole moment, *Geochem. Geophys. Geosyst.,* **9,** Q04038.

Goguitchaichvili, A., Greco, C. & Morales, J., 2011. Geomagnetic field intensity behavior in South America between 400 AD and 1800 AD: first archeointensity results from Argentina, *Phys. Earth planet. Inter.,* **186,** 191–197.

Goguitchaichvili, A., Laponte, D., Morales, J. & Acosta, A., 2012. Archaeointensity of the Earth's magnetic field retrieved from Pampean Ceramics (South America), *Archaeometry,* **54**(2), 213–224.

Gómez-Paccard, M. *et al.*, 2006. A catalogue of Spanish archaeomagnetic data, *Geophys. J. Int.,* **166,** 1125–1143.

Gómez-Paccard, M., Chauvin, A., Lanos, Ph. & Thiriot, J., 2008. New archaeointensity data from Spain and the geomagnetic dipole moment in western Europe over the past 2000 years, *J. geophys. Res.,* **113,** B09103.

Halgedahl, S.L., Day, R. & Fuller, M., 1980. The effect of cooling rate intensity of week-field TRM in single-domain magnetite, *J. geophys. Res.,* **85,** 3690–3698.

Hedley, I. & Wagner, G.C., 1991. A magnetic investigation of Roman and pre-Roman pottery, in *Archaeometry '90,* pp. 275–284, eds Pernicka, E. & Wagner, G.C., Birkhaeuser, Basel.

Jackson, A., Jonkers, A. & Walker, M., 2000. Four centuries of geomagnetic secular variation from historical records, *Philos. Trans. R. Soc. Lond., A,* **358,** 957–990.

Korte, M. & Constable, C.G., 2005. Continuous geomagnetic field models for the past 7 millennia: 2.CALS7K, *Geochem. Geophys. Geosyst.,* **6,** Q02H16.

Korte, M. & Constable, C.G., 2011. Improving geomagnetic field reconstructions for 0–3 ka, *Phys. Earth planet. Inter.,* **188,** 247–259.

Korte, M., Genevey, A., Constable, C., Frank, U. & Schnepp, E., 2005. Continuous geomagnetic field models for the past 7 millennia: 1. A new global data compilation, *Geochem. Geophys. Geosyst.,* **6,** Q02H15.

Korte, M., Donadini, F. & Constable, C.G., 2009. Geomagnetic field for 0–3 ka: 2. A new series of time-varying global models, *Geochem. Geophys. Geosyst.,* **10,** Q06008.

Korte, M., Constable, C.G., Donadini, F. & Holme, R., 2011. Reconstructing the Holocene geomagnetic field, *Earth planet. Sci. Lett.,* **312,** 497–505.

Kosterov, A.A., Perrin, M., Glen, J.M. & Coe, R.S., 1998. Paleointensity of the Earth's magnetic field in Early Cretaceous time: the Parana Basalt, Brazil, *J. geophys. Res.,* **103,** 9739–9753.

Lanza, R. & Zanella, E., 2003. Palaeomagnetic secular variation at Vulcano (Aeolian Islands) during the last 135 kyr, *Earth planet. Sci. Lett.,* **213,** 312–336.

Levi, S., 1977. The effect of magnetite particle size on paleointensity determinations of the geomagnetic field, *Phys. Earth planet. Inter.,* **13,** 245–259.

Lowrie, W., 1990. Identification of ferromagnetic minerals in a rock by coercivity and unblocking temperature properties, *Geophys. Res. Lett.,* **17,** 159–162.

McClelland-Brown, E., 1984. Experiments on TRM intensity dependence on cooling rate, *Geophys. Res. Lett.,* **11**(3), 205–208.

Morales, J., Goguitchaichvili, A., Acosta, G., González-Morán, T., Alva-Valdivia, L., Robles-Camacho, J. & Hernández-Bernal, M.S., 2009. Magnetic properties and archeointensity determination on Pre-Columbian pottery from Chiapas, Mesoamerica, *Earth Planets Space,* **61,** 83–91.

Néel, L., 1949. Théorie du traînage magnétique des ferromagnétiques en grains fins avec applications aux terres cuites, *Ann. Géophys.,* **5,** 99–136.

Pavón-Carrasco, F.J., Osete, M.L., Torta, J.M. & Gaya-Piqué, L.R., 2009. A regional archaeomagnetic model for Europe for the last 3000 years, SCHA.DIF.3K: applications to archaeomagnetic dating, *Geochem. Geophys. Geosyst.,* **10**(3), Q03013.

Schnepp, E., Pucher, R., Reindeers, J., Hambach, U., Soffel, H. & Hedley, I., 2004. A German catalogue of archaeomagnetic data, *Geophys. J. Int.,* **157,** 64–78.

Selkin, P. & Tauxe, L., 2000. Long-term variations in palaeointensity, *Phil. Trans. R. Soc. Lond.,* **358,** 1065–1088.

Tema, E., 2011. Archaeomagnetic research in Italy: recent achievements and future perspectives, in *The Earth's Magnetic Interior,* IAGA Special Sopron Book Series, Vol. 1, Chapter 15, pp. 213–233, eds Petrovsky, E., Herrero-Bervera, E., Harinarayana, T. & Ivers, D., Springer.

Tema, E. & Kondopoulou, D., 2011. Secular variation of the Earth's magnetic field in the Balkan region during the last 8 millennia based on archaeomagnetic data, *Geophys. J. Int.,* **186,** 603–614.

Tema, E., Hedley, I. & Lanos, Ph., 2006. Archaeomagnetism in Italy: a compilation of data including new results and a preliminary Italian secular variation curve, *Geophys. J. Int.,* **167,** 1160–1171.

Tema, E., Goguitchaichvili, A. & Camps, P., 2010. Archaeointensity determinations from Italy: new data and the Earth's magnetic field strength variation over the past three millennia, *Geophys. J. Int.,* **180,** 596–608.

Tema, E., Gómez-Paccard, M., Kondopoulou, D. & Ylenia, A., 2012. Intensity of the Earth's magnetic field in Greece during the last five millennia: new data from Greek pottery, *Phys. Earth planet. Inter.,* **202–203,** 14–26.

Tema, E. *et al.*, 2013. Combined archaeomagnetic and thermoluminescence study of a brick kiln excavated at Fontanetto Po (Vercelli, Northern Italy), *J. Archaeol. Sci.,* **40,** 2025–2035.

Thellier, E. & Thellier, O., 1959. Sur l'intensité du champ magnétique terrestre dans le passé historique et géologique, *Ann. Geophys.,* **15,** 285–376.

Valet, J.P., Herrero-Bervera, E., LeMouël, J.L & Plenier, G., 2008. Secular variation of the geomagnetic dipole during the past 2000 years, *Geochem. Geophys. Geosyst.,* **9,** Q01008.

Veitch, R.J., Hedley, I.G. & Wagner, J.J., 1984. An investigation of the intensity of the geomagnetic field during Roman times using magnetically anisotropic bricks and tiles, *Arch. Sci. (Geneva),* **37**(3), 359–373.